35th Annual International Conference of the IEEE EMBS
Osaka, Japan, 3 - 7 July, 2013

A Regularization-Free Young's Modulus Reconstruction Algorithm for Ultrasound Elasticity Imaging

Xiaochang Pan, Jing Gao, Jinhua Shao, Jianwen Luo, *Member, IEEE*, and Jing Bai, *Fellow, IEEE*

***Abstract*—Ultrasound elasticity imaging aims to reconstruct the distribution of elastic modulus (e.g., Young's modulus) within biological tissues, since the value of elastic modulus is often related to pathological changes. Currently, most elasticity imaging algorithms face a challenge of choosing the value of the regularization constant. We propose a more applicable algorithm without the need of any regularization. This algorithm is not only simple to use, but has a relatively high accuracy. Our method comprises of a nonrigid registration technique and tissue incompressibility assumption to estimate the two-dimensional (2D) displacement field, and finite element method (FEM) to reconstruct the Young's modulus distribution. Simulation and phantom experiments are performed to evaluate the algorithm. Simulation and phantom results showed that the proposed algorithm can reconstruct the Young's modulus with an accuracy of 63~85%.**

I. Introduction

Ultrasound elasticity imaging has received much attention in the past two decades. It can provide mechanical property (e.g., elasticity or elastic modulus, such as Young's modulus) information and help distinguish diseased part from normal soft tissue. Elastography using a quasi-static compression [1] is the most established approach. It typically estimates the strain within the tissue, which could be interpreted as an indirect measure of Young's modulus distribution, under the assumption of a constant stress field within the tissues [1]. However, the stress within the tissues decreases with depth and concentrates at the boundaries of inclusions [1]. The assumption of constant stress induces artifact which may compromise the diagnostic quality [2]. Consequently, many researchers are devoted to the reconstruction of elasticity distribution [2-6].

The reconstruction of elasticity is an inverse problem [4]. Most inversion schemes assume that tissues are linear elastic, isotropic, continuous and incompressible [2-5]. Besides, most researchers reduce the three-dimensional (3D) elasticity problem to a two-dimensional (2D) problem, using either a plane-strain [2] or plane-stress [6] approximation. The relative Young's modulus can be reconstructed from the displacement field by either direct or iterative methods. The iterative method is found to be more robust than the direct method [4]. However, a regularization term is needed, and the value of the regularization parameter has significant effects on the reconstruction results [7]. It is difficult to obtain the optimal regularization parameter in practice.

The purpose of this study is to develop a more applicable algorithm that does not need any regularization. Meanwhile our algorithm still possesses acceptable reconstruction accuracy. In this paper, the nonrigid registration technique based on the B-spline model [8] and tissue incompressibility assumption [9] are used to estimate the 2D displacement field. Then, the finite element method is used to reconstruct the Young's modulus. The proposed method is tested in simulation and experiments on standard elasticity phantoms.

II. Methods

A. Displacement estimation

Precise calculation of displacement field is the foundation of elasticity imaging [7]. Suppose the pre- and post-deformed RF signals are $I_1(\mathbf{x},\mathbf{y})$ and $I_2(\mathbf{x},\mathbf{y})$, where $\boldsymbol{x}$ and $\boldsymbol{y}$ stand for axial (i.e., along the ultrasound beams) and lateral (i.e., perpendicular to the ultrasound beams and in the imaging plane) directions, respectively. Axial displacement $\mathbf{v}(\mathbf{x},\mathbf{y})$ and lateral displacement $\mathbf{u}(\mathbf{x},\mathbf{y})$ are the variables to be calculated. Under the assumption of a plane strain problem, the displacement in the elevation direction (i.e., perpendicular to the imaging plane) is zero. The nonrigid registration technique based on the B-splines model, previously used in MRI [8] and ultrasound [10] image registration, was utilized in this study to estimate 2-D displacement field. The main idea of this approach is to deform $I_1(\mathbf{x},\mathbf{y})$ by B-splines to approximate $I_2(\mathbf{x},\mathbf{y})$ as much as possible.

We denote $a_{i,j}$ with size of $n_x \times n_y$ as axial displacement's parameter, and denote $b_{i,j}$ with the same size as lateral displacement's parameter. n_x and n_y are the respective number of uniformly-spaced knots in the lateral and axial directions, respectively. Then, the axial and lateral displacement fields can be presented as

$$\mathbf{v}(x,y)=\sum_{m=0}^{3}\sum_{n=0}^{3}a_{i+m,j+n}B_m(p)B_n(q) \qquad (1)$$

* Research supported by the National Basic Research Program of China (973) under Grant No. 2011CB707701, the National Natural Science Foundation of China under Grant No. 81227901, 81071191, 81271617, 81201160 and 61271131, the National Major Scientific Instrument and Equipment Development Project under Grant No. 2011YQ030114, National Science and Technology Support Program under Grant No. 2012BAI23B00 , Tsinghua University Initiative Scientific Research Program and Tsinghua National Laboratory for Information Science and Technology（TNList）Cross-discipline Foundation.

X. Pan, Jinhua Shao, J. Luo and J. Bai are with the Department of Biomedical Engineering, School of Medicine, Tsinghua University, Beijing 100084, CHINA (e-mail: deabj@tsinghua.edu.cn).

J. Luo and J. Gao are also with the Center for Biomedical Imaging Research, Tsinghua University , Beijing 100084, CHINA (e-mail: luo_jianwen@tsinghua.edu.cn).

$$\mathbf{u}(x,y)=\sum_{m=0}^{3}\sum_{n=0}^{3}b_{i+m,j+n}B_m(p)B_n(q) \quad (2)$$

where $i=[x/n_x]-1$, $j=[y/n_y]-1$, $p=x/n_x-[x/n_x]$, $q=y/n_y-[y/n_y]$ and B_m stands for the m-th basis function of the B-spline. The nonrigid registration algorithm is a typical optimization technique which minimizes the cost function with respect to the estimated displacement. The sum of squared differences (SSD) criterion [10] is chosen as the cost function here.

$$C=\sum(I_1(\mathbf{x},\mathbf{y})-I_2(\mathbf{x}+\mathbf{u},\mathbf{y}+\mathbf{v}))^2 \quad (3)$$

The parameters $a_{i,j}$ and $b_{i,j}$ are optimized with Gauss-Newton method to minimize the cost function C. Both axial and lateral displacements are then calculated from Eqs. (1) and (2). However, the lateral displacement estimation is much noisier than the axial one, due to lower resolution, lower sampling frequency and lack of phase information in the lateral direction [9] [11]. The assumption of 2D plane strain and incompressibility is then used to estimate more accurate lateral displacement, by utilizing the constraint condition [9]

$$\frac{\partial u}{\partial x}+\frac{\partial v}{\partial y}=0 \quad (4)$$

The term $\frac{\partial v}{\partial y}$ can be obtained from the partial derivative of Eq. (1). Combing Eq. (4) and the partial derivative of Eq. (2), the lateral displacement's parameters $b_{i,j}$ are then calculated using the least squares technique. Finally, the lateral displacement is obtained by substituting $b_{i,j}$ into Eq. (2).

B. Elasticity reconstruction

The estimated displacement field is used as the input of the elasticity reconstruction algorithm. Nevertheless, the elasticity cannot be derived by the displacement field alone [12]. Either the stress distribution or the elastic modulus must be measured along a sufficient portion of the boundary [12]. The Young's moduli around a region of interest (ROI) are assumed to be an arbitrary constant in our model [13]. Uniform rectangular elements are used in our FEM inversion model. Boundary node forces are calculated firstly by solving a 2D forward problem. The elastic moduli of elements around the boundary of ROI are set to an arbitrary constant (1 in our model). The Poisson ratio is set to be 0.495 throughout the ROI under the near-incompressibility assumption [2].

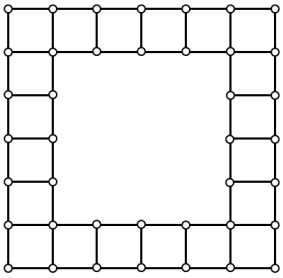

Figure 1. Elements around the boundary of ROI.

Considering these elements alone as an object (Fig. 1), the node forces can be calculated by

$$\mathbf{K}_{boundary}\mathbf{d}_{boundary}=\mathbf{f} \quad (5)$$

where $\mathbf{K}_{boundary}$, $\mathbf{d}_{boundary}$, and $\mathbf{f}$ are the global stiffness matrix, the global nodal displacement vector and the global nodal force vector of boundary, respectively. Node displacement $\mathbf{d}_{boundary}$ can be obtained from the estimated displacement field. $\mathbf{K}_{boundary}$ can be assembled by each element with the known node position, Young's modulus and Poisson ratio.

Then, the Young's modulus distribution within the ROI is calculated by solving an inverse problem. Unlike the forward problem in the FEM, the Young's modulus of each element becomes unknown in the inverse problem. Hence, the Young's modulus vector $\mathbf{E}$ is the variable to be solved. Now, consider all the elements within the ROI as an object. Denote the number of elements and nodes as $N_{element}$ and N_{node}, respectively. Extract Young's modulus vector $\mathbf{E}$ from the multiplication of the global stiffness matrix $\mathbf{K}_{roi}$ and the displacement vector $\mathbf{d}$. The left term of Eq. (5) becomes

$$\mathbf{K}_{roi}\mathbf{d}=\mathbf{D}\mathbf{E} \quad (6)$$

Here, the size of $\mathbf{D}$ is $2N_{node}\times N_{element}$, while the size of $\mathbf{E}$ is $N_{element}\times 1$. For more details about the procedure of assembly of matrix $\mathbf{D}$, readers can refer to [5]. For the quadrilateral element used in this method, N_{node} is greater than $N_{element}$. The Young's modulus vector $\mathbf{E}$ is solved by the least square method

$$\mathbf{E}=(\mathbf{D}^T\mathbf{D})\setminus\mathbf{D}^T\mathbf{f}_{boundary} \quad (7).$$

The boundary nodal force vector $\mathbf{f}_{boundary}$ is a subset of $\mathbf{f}$ which has been solved in (5).

III. Results and Discussion

A. Simulation Study

To evaluate our algorithm, a model with known elastic moduli was simulated with finite element analysis software (FEMLAB 2.3, Comsol Inc. Burlington, MA). The model was linear elastic, isotropic, incompressible and in plane strain state [2, 4]. Three inclusions with diameter of 5mm were simulated. The Young's moduli of the inclusions and the background were 60 KPa and 20 KPa, respectively. The whole size of simulated images was 38 mm×38 mm.

A 1% axial compression was applied to the model, with a perfect slip boundary. Randomly-distributed ultrasound scatterers were simulated within the ROI, and then the displacements of all the scatterers were calculated from finite element analysis. Consequently, the pre- and post-deformed RF signals were simulated using Field II simulation software [14]. A linear array was simulated, with a 10 MHz center frequency and 32 MHz sampling frequency.

The displacement fields are calculated from the simulated RF signals using nonrigid registration. The errors of axial and lateral displacement are 0.0025 ± 0.0010 and 0.0128 ± 0.0039 mm (mean ± standard deviation), respectively. The result of the displacement has both advantages of high precision and

smoothness, partially due to the use of the B-Spline model, as precise displacement estimation is the foundation of elasticity reconstruction [7].

Figure 2 compares the simulated and reconstructed relative Young's modulus distribution. The theoretical relative modulus of inclusions is 3. The mean value of reconstructed modulus of the inclusions is 1.89, and the standard deviation is 0.49. The error of reconstructed relative Young's modulus of the whole image is 0.18 ± 0.35 (mean ± standard deviation).

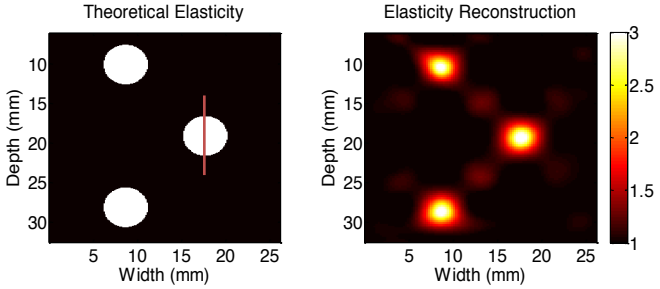

Figure 2. The true relative moduli in simulation (left) and the relative moduli reconstructed with FEM inversion method (right).

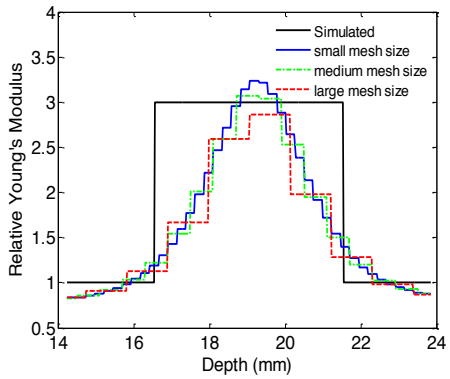

Figure 3. Reconstructed Young's moduli of different mesh size with theoretical value along the line A-A'.

Figure 3 shows the comparison of reconstructed Young's moduli of different mesh sizes with theoretical value along the line A-A' (Fig. 2). The mesh sizes are 0.24×0.24, 0.60×0.60, 1.10×1.10mm^2 (height×width), respectively. The reconstructed moduli of inclusions are 1.89±0.16, 1.86±0.16, 1.80±0.15. A lager mesh size induces less accuracy.

B. Phantom Study

Experiments were performed on a tissue mimicking elasticity QA phantom (model 049A, CIRS Inc., Norfolk, VA, USA) (Fig. 4). The Young's moduli of inclusions and background were 80±12 KPa and 25±6 KPa, respectively. Experiments on two different moduli of inclusions were also studied on a multi-purpose tissue mimicking phantom (model 040GSE) (Fig. 6). The Young's moduli of the inclusions were 40 KPa and 60 KPa, respectively. The background's modulus was 24 KPa. The material of these two phantoms was described as solid-elastic with tissue-like acoustic properties. The raw RF signals were recorded at a sampling frequency of 32 MHz with an iU22 ultrasound system (Philips Medical Systems, Bothell, WA, USA), equipped with an L9-3 linear array transducer.

Figure 4. Elasticity QA phantom used in our experiment.

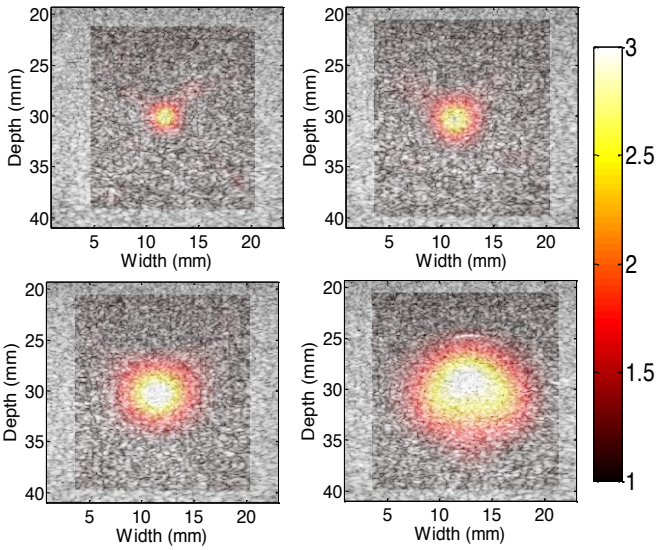

Figure 5. The reconstructed relative Young's moduli overlaid onto the B-mode images with four different sizes of inclusions.

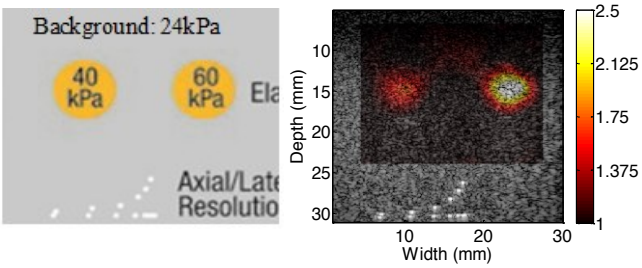

Figure 6. The selected ROI of the multi-purpose phantom (model 040GSE) (left), and the reconstructed relative Young's moduli (right).

Figure 5 shows the relative Young's modulus reconstruction results of 4 different inclusions with diameter of 2.5 mm, 4.1 mm, 6.5 mm and 10.4 mm, respectively. The inclusions' positions in the reconstruction results fit well with the B mode images. However, one of the drawbacks of this algorithm is the smoothing effect of the modulus value. For further analysis of the reconstructed modulus value, we manually segmented the inclusions on the B-mode images, and quantitatively compared the relative Young's moduli of these inclusions with the reference values (i.e., 3.2).

For the phantom model 049A (Fig. 5), The four inclusions' relative Young's moduli are reconstructed as 2.44 ± 0.19, 2.45 ± 0.22, 2.63 ± 0.28, 2.71 ± 0.25 (mean value ± standard deviation) corresponding to the diameters of 2.5 mm, 4.1 mm, 6.5 mm and 10.4 mm, respectively. The reference relative

Young's moduli of inclusions are approximately 3.2. For the phantom model 040GSE (Fig. 6), the two inclusions' relative Young's moduli are reconstructed as 1.40 ± 0.16 and 2.12 ± 0.29 corresponding to the reference value of approximately 1.67 and 2.5, respectively.

However, one drawback of this algorithm was the smoothing effect of the inclusions' edge on the reconstructed modulus image. The reasons of the smoothing effect lie in two aspects. Firstly, the modulus is related to strain tensors and their derivatives [6]. The displacements obtained from nonrigid registration are low-pass filtered. The high-frequency noises together with high-frequency strain information are filtered out. So the high-frequency components in the modulus distribution are eliminated. The edges of inclusions related to the high-frequency components are therefore smoothed. Secondly, the strain is assumed to be linear within each element in our finite element inversion model. The high-frequency components of strain have not been taken into consideration. These two aspects lead to the reconstruction results' smoothing effect and resultant lower reconstruction value than true value of inclusions.

The experiments showed that our algorithm is capable of reconstructing the relative moduli of more than one inclusion, with the same (Fig. 2) or different moduli (Fig. 6). The relative Young's moduli reconstructed with our algorithm are close to or slightly better than those with the iterative method using regularization [7]. Yet, without regularization and iteration, our method is not only simple to use, but also fast. The reconstruction time of each image is less than 30 sec in Matlab (MathWorks, Inc., Natick, MA, USA). These advantages make our algorithm more applicable in practice.

We applied the nonrigid registration technique with B-splines model to ultrasound RF signals, instead of B-mode images [10]. RF signals are known to provide a high resolution, accuracy and precision in displacement estimation [1]. In order to avoid the local minima of the optimization process of displacement estimation, an initial displacement is required to start optimization. We utilized the cross-correlation technique [1] to obtain the coarse displacement as the initial displacement for the optimization process.

Besides the estimated displacement, the size of the element also influences the result of elasticity reconstruction. The element of 0.24×0.24 mm^2 is used in both simulation and phantom experiments. As shown in Fig. 3, the smaller the size of element is, the more precise and smoother elasticity can be reconstructed. However, the use of a smaller element size costs more computation time and memory space. We should choose a suitable element size to balance the reconstruction precise and computation time.

There is no known boundary force or Young's modulus used in our algorithm, so we can only reconstruct the relative, rather than absolute, Young's modulus [12]. Nevertheless, another feature of our algorithm is no need to concern the boundary force. This avoids the errors introduced by the assumption of zero normal traction in the boundaries [4, 7]. However, when the Young's moduli on the edge of ROI are not equal, our algorithm may cause certain error. Such error could be minimized by carefully choosing the ROI on B-mode and/or strain images.

IV. Conclusion

In this study, we develop a more applicable modulus reconstruction method for ultrasound elasticity imaging. We utilize B-spline based nonrigid registration technique and tissue incompressibility to estimate 2D displacement from ultrasound RF signals. After calculated, the displacements are used to reconstruct each element's Young's modulus with FEM. Each element's relative modulus value can be directly obtained without any regularization. The results of simulation and phantom experiments suggest that this algorithm is applicable and can provide accurate results. Future work will involve the improvement of the accuracy of our algorithm and application of the proposed algorithm in in-vivo experiments on human subjects.

V. References

[1] J. Ophir, I. Cespedes, H. Ponnekanti, Y. Yazdi, and X. Li, "Elastography: a quantitative method for imaging the elasticity of biological tissues," Ultrasonic imaging, vol. 13, pp. 111-134, 1991.

[2] F. Kallel and M. Bertrand, "Tissue elasticity reconstruction using linear perturbation method," Medical Imaging, IEEE Transactions on, vol. 15, pp. 299-313, 1996.

[3] M. Doyley, P. Meaney, and J. Bamber, "Evaluation of an iterative reconstruction method for quantitative elastography," Physics in Medicine and Biology, vol. 45, p. 1521, 2000.

[4] A. A. Oberai, N. H. Gokhale, and G. R. Feijóo, "Solution of inverse problems in elasticity imaging using the adjoint method," Inverse Problems, vol. 19, p. 297, 2003.

[5] Y. Zhu, T. J. Hall, and J. Jiang, "A finite-element approach for Young's modulus reconstruction," Medical Imaging, IEEE Transactions on, vol. 22, pp. 890-901, 2003.

[6] C. Sumi, A. Suzuki, and K. Nakayama, "Estimation of shear modulus distribution in soft tissue from strain distribution," IEEE Trans Biomed Eng, vol. 42, pp. 193-202, Feb 1995.

[7] M. S. Richards, P. E. Barbone, and A. A. Oberai, "Quantitative three-dimensional elasticity imaging from quasi-static deformation: a phantom study," Phys Med Biol, vol. 54, pp. 757-79, Feb 7 2009.

[8] D. Rueckert, L. I. Sonoda, C. Hayes, D. L. G. Hill, M. O. Leach, and D. J. Hawkes, "Nonrigid registration using free-form deformations: application to breast MR images," Medical Imaging, IEEE Transactions on, vol. 18, pp. 712-721, 1999.

[9] M. A. Lubinski, S. Y. Emelianov, K. Raghavan, A. E. Yagle, A. R. Skovoroda, and M. O'Donnell, "Lateral displacement estimation using tissue incompressibility," Ultrasonics, Ferroelectrics and Frequency Control, IEEE Transactions on, vol. 43, pp. 247-256, 1996.

[10] M. J. Ledesma-Carbayo, J. Kybic, M. Desco, A. Santos, M. Suhling, P. Hunziker, et al., "Spatio-temporal nonrigid registration for ultrasound cardiac motion estimation," IEEE Trans Med Imaging, vol. 24, pp. 1113-26, Sep 2005.

[11] J. Luo and E. E. Konofagou, "Effects of various parameters on lateral displacement estimation in ultrasound elastography," Ultrasound in medicine & biology, vol. 35, pp. 1352-1366, 2009.

[12] P. E. Barbone and J. C. Bamber, "Quantitative elasticity imaging: what can and cannot be inferred from strain images," Physics in medicine and biology, vol. 47, p. 2147, 2002.

[13] A. Skovoroda, S. Emelianov, and M. O'Donnell, "Tissue elasticity reconstruction based on ultrasonic displacement and strain images," Ultrasonics, Ferroelectrics and Frequency Control, IEEE Transactions on, vol. 42, pp. 747-765, 1995.

[14] J. A. Jensen, "Field: A program for simulating ultrasound systems," Medical and Biological Engineering and Computing, vol. 34, pp. 351-352, 1996.